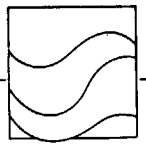

Mediterranean deep water formation baroclinic instability and oceanic eddies

Deep water formation
Baroclinic instability
Eddies
North-Western Mediterranean Sea
Medoc 1975
Formation des eaux profondes
Instabilité barocline
Tourbillons
Méditerranée nord-occidentale
Medoc 1975

J. C. Gascard
Laboratoire d'Océanographie Physique du Muséum National d'Histoire Naturelle, 43, rue Cuvier, 75231 Paris.

Received 29/11/77, in revised form 16/2/78, accepted 28/3/78

ABSTRACT

Since 1969 in studying formation of deep water in the North Western Mediterranean Sea in winter, we discovered frequent cyclonic and anticyclonic eddies genesis associated with processes of deep water formation. We are now presenting such typical eddies observed in February-March 1975, during the Medoc 75 cruise (Medoc area: 3°30′ E-6°E, and 41°N-43°N). Vertical speed has also been measured in this area. Since several orders of magnitude appear from these measurements, it may be supposed that several dynamical processes are present in deep water formation. We will show that baroclinic instability, which is one of these processes, is responsible for that part of the slow (1 mm . s^{-1}) and aperiodic vertical motions, and corresponds to meanders, eddies and fronts on the horizontal plane. Considering the observations which allow us to use a quasi-geostrophic approximation, we will propose a baroclinic instability model in order to explain the features of these three-dimensional motions. We will evaluate the importance of the mixing induced by this mechanism in the process of deep water formation between surface and subsurface waters under the meteorological forcing.

Oceanol. Acta, **1**, 3, 1978, 315-330.

RÉSUMÉ

La formation des eaux profondes méditerranéennes instabilité barocline et tourbillons océaniques

Les études que nous avons entreprises depuis 1969, dans le but de mieux comprendre les mécanismes qui gouvernent la formation des eaux profondes méditerranéennes au large du Golfe du Lion, nous ont conduit à découvrir dans cette région de l'océan l'existence en hiver de petits tourbillons cycloniques et anticycloniques associés par paires. Nous présentons dans cet article un exemple type de tels tourbillons, observé en février-mars 1975 au cours de la campagne Medoc 75 (aire Medoc : 3°30′E à 6°E et 41°N à 43°N). Plusieurs processus dynamiques de nature différente interviennent dans la formation de ces eaux profondes puisque des mouvements verticaux sont observés en période de formation à des échelles de temps et d'espace distinctes. Nous présentons, dans le cadre de l'approximation quasi-géostrophique, un modèle des mouvements tridimensionnels d'échelle moyenne, qui correspondent dans le plan vertical à des mouvements lents (1 mm . s^{-1}) et apériodiques, qui apparaissent dans le plan horizontal sous la forme de méandres puis de tourbillons et de fronts et qui résultent du mécanisme de l'instabilité barocline. Tenant compte des observations faites de Medoc 69 à Medoc 75, nous évaluons l'importance que ce mécanisme peut avoir dans le processus de formation des eaux profondes méditerranéennes à partir de la transformation et du mélange des eaux de surface et des eaux intermédiaires subsuperficielles sous l'effet des conditions atmosphériques.

Oceanol. Acta, **1**, 3, 1978, 315-330.

INTRODUCTION

The North-Western Mediterranean basin is characterized at all seasons by a large cyclonic, thermohaline circulation of superficial water masses coming from the Atlantic Ocean, and subsuperficial water masses deriving from the eastern Mediterranean "Levantine Water", above a thick deep water layer (1 500 to 2 000 m) (Nielsen, 1912). The Levantine Water, formed around the islands of Rhodes and Cyprus, is revealed by a T(°C) and S(‰) maximum at a depth of about 150-300 m. After mixing with other water masses, it passes westwards through the Strait of Sicily, and is present, in all the western basin, in the Intermediate Water layer. The circulation of this Intermediate Water, which, after passing through the Strait of Sardinia, flows geostrophically northwards along the Sardinian and Corsican coasts, is partly the cause of the North-Western Mediterranean cyclonic circulation.

Another cause would be the water level difference on either side of the Strait of Gibraltar (Lacombe, Tchernia, 1972).

As is well known, the Medoc area (41° to 43°N, 3°30 to 6°E) is generally occupied by a three-layer system which consists of:

– a *surface layer*, some 100 m in depth, limited downwards by a small temperature minimum, and which, in winter (February, March), has the following characteristics:
$\theta°C \simeq 12.5\text{-}12.6$;
$38.10 < S‰ < 38.25$;
$28.90 < \sigma_\theta < 29.04$;

– an *intermediate layer* (IW), relatively warm and salty:
$13.20 < \theta°C < 13.30$;
$38.50 < S‰ < 38.55$;
$29.08 < \sigma_\theta < 29.10$;

– a *deep layer*, below 800 m: $\theta°C \simeq 12.7$; $S‰ \simeq 38.41$; $\sigma_\theta \simeq 29.11$.

The maximum values of θ°C and S‰ within the Intermediate Water provide a "Hook" in the θ.S diagrams.

During the summer the 3-layer stratified water masses flow along the continental slope of the Gulf of Lions into the Balearic Sea.

In winter, they deviate from the continental slope off the "Cap de Creux" and then flow eastwards at latitude 41°30'N. A vortex (cyclonic gyre) appears, 100 km in diameter, with its center at 42°N-4°45'E.

The general cyclonic motion separates heavy waters in the center from light waters at the periphery, and induces a horizontal divergence at the surface and a convergence in depth, so that vertical motions occur in the center. From the periphery to the center appears a progressive slope of the isopycnals towards the surface. A common feature is that, on vertical sections, isolines show a central doming (Tchernia, Fieux, 1971). The pycnocline is situated at about 100 m depth in the center, and is 3 or 4 times deeper 50 km farther. In the center, the vertical stratification decreases, but remains stable. During the winter, the area is subjected to the effect of strong, cold, dry, continental winds blowing from NW to N (Mistral, Tramontane). High evaporation and strong cooling act efficiently to reduce the stability of the central part of the surface layer since, on the one hand, these slightly moving water masses, are longer exposed to the atmospheric effects than the peripheric water masses, which move faster all around the basin, and, on the other hand, these superficial water masses are 3 or 4 times less thick in the center than at the periphery.

This preconditioning effect is, however, noticeable after a certain time, for when the Mistral is blowing, the density increase of the superficial waters appears to be uniform throughout the whole basin (Stommel, 1972).

The winter observations show that the Intermediate Water layer is still present at the periphery, whereas, in the central area, the 3-layer system disappears and a quasi-homogeneous layer exists through the whole water column (chimney), since the surface density (Fig. 1) exceeds 29.0 in σ_θ. On the edge of this homogeneous water, a "front" is present (Fig. 2). The intersection of this front with the surface appears more or less clearly as a wave-shaped curve or meanders characterized by a wavelength of approximately 40 km.

Up to day, many other winter features have been recognised in this Medoc area such as fronts, eddies and "chimneys". We will present (p. 317) some new recent observations made during Medoc 75.

In 1970, the Medoc Group proposed a first general description of Mediterranean deep water formation, divided into three different consecutive phases: preconditioning, violent mixing and sinking + spreading. Similar more detailed descriptions have been proposed by Lacombe et Tchernia (1972) and Sankey (1973). More specifically, Stommel (1972), Swallow and Caston (1973) and Hogg (1973) have proposed detailed explanations of the preconditioning phase, that means erosion of the upper layer vertical stratification. Anati (1971) and Killworth (1976) have suggested a two-dimensional non-penetrative convection model for the violent mixing phase induced by meteorological forcing, while Saint-Guily (1972) and Gascard (1973) have studied turbulent mixing induced by the breaking of large-amplitude internal waves. The very intense vertical motions observed in the Medoc area (up to 10 cm.sec^{-1}) would be caused by these waves.

Killworth (1976) considered the final phase, i.e. the sinking and spreading of dense and homogeneous waters formed during the second phase, to be a result of a baroclinic instability mechanism producing small eddies (10 km in diameter) observed in the Medoc area. He demonstrated this fact using a peculiar model based on a quasi-geostrophic approximation within a homogeneous fluid; so, he had to take into account *viscosity* in order "to avoid spurious growing solutions". Killworth also showed that baroclinic instability of this type can only occur in alternance with non-penetrative convection. The convection from the surface cooling swamps the baroclinic instability.

We will present (p. 323) a more classical two-layer baroclinic instability model – such as described by Tang

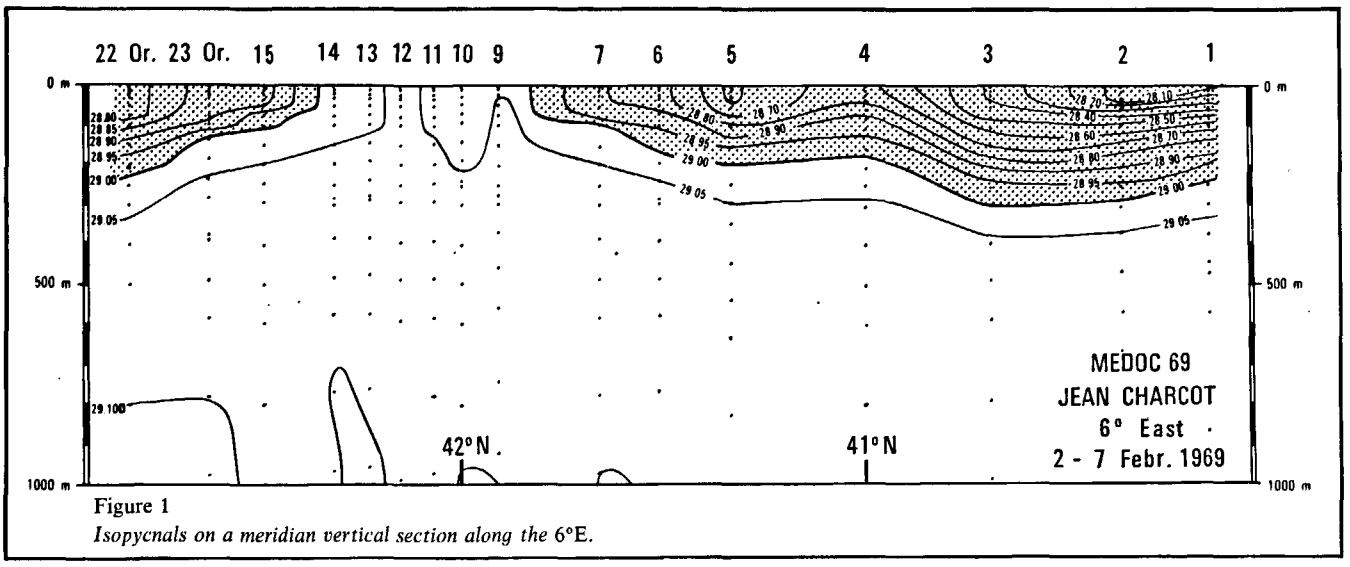

Figure 1
Isopycnals on a meridian vertical section along the 6°E.

(1975), but *with conservation of the Rossby internal radius of deformation*, and we will show that there is generally good agreement between the theoretical results obtained from this model and the observations described (p. 317).

We will pay particular attention to the *mixing induced by this instability mechanism* which tends to weaken the vertical stratification and makes convection triggered from the surface more efficient.

We will then propose (p. 328) a *descriptive model* for the formation of Mediterranean deep waters, considering that the mixing phase is partly and alternatively due to *convective processes* (buoyancy subrange) and *advective processes* (rotational subrange), resulting in two types of deep waters such as revealed by observations.

MEDOC OBSERVATIONS

Hydrology and horizontal motions of Medoc 75

During 1975, we were able to follow both the evolution of the hydrology and the dynamic situation in the Medoc area.

This evolution may be divided into two periods:

FIRST PERIOD: 18-27 FEBRUARY, 1975

A 25 nautical miles zone, centered at 42°05'N-4°30'E is explored with a bathysonde (Fig. 3).

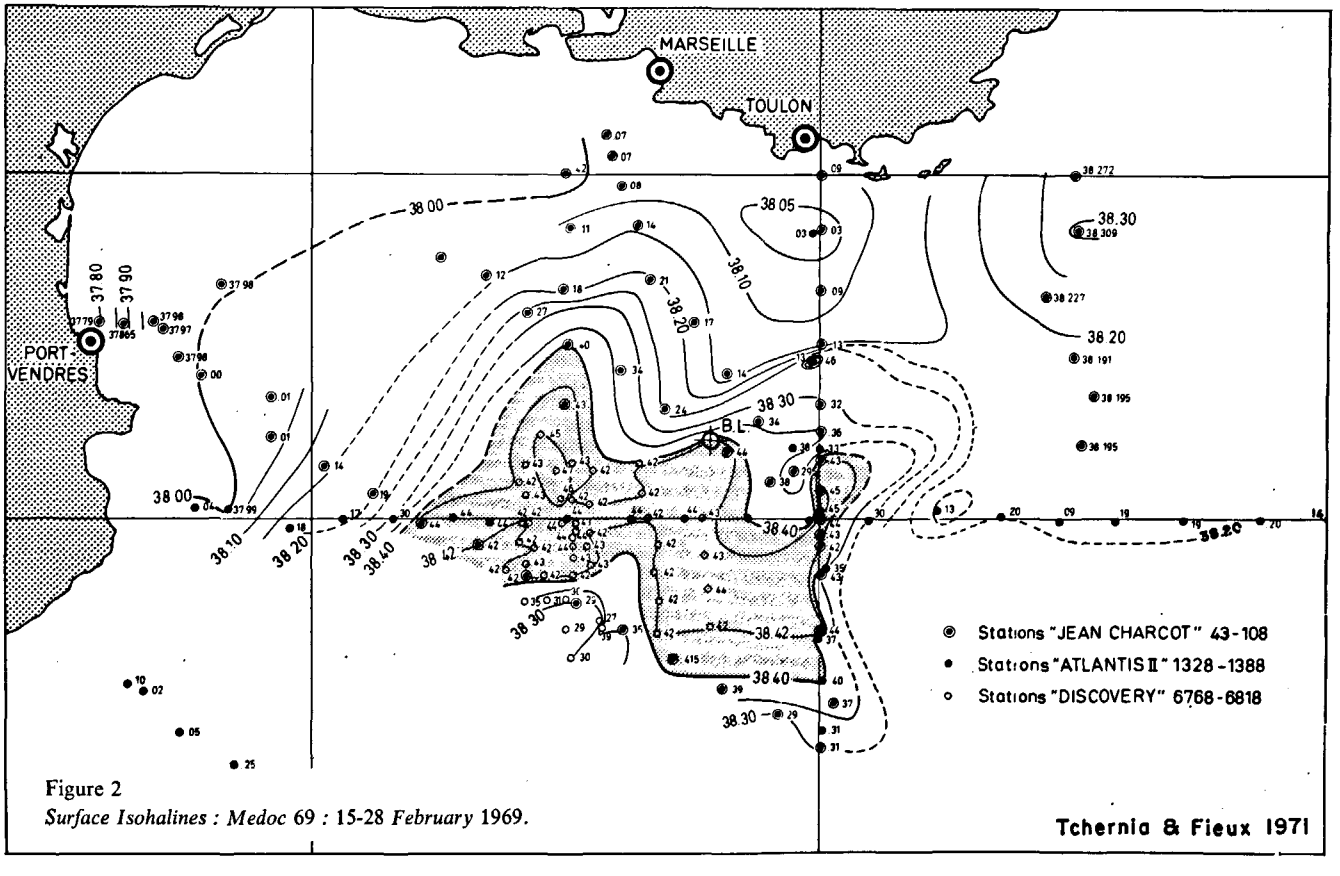

Figure 2
Surface Isohalines : Medoc 69 : 15-28 February 1969.

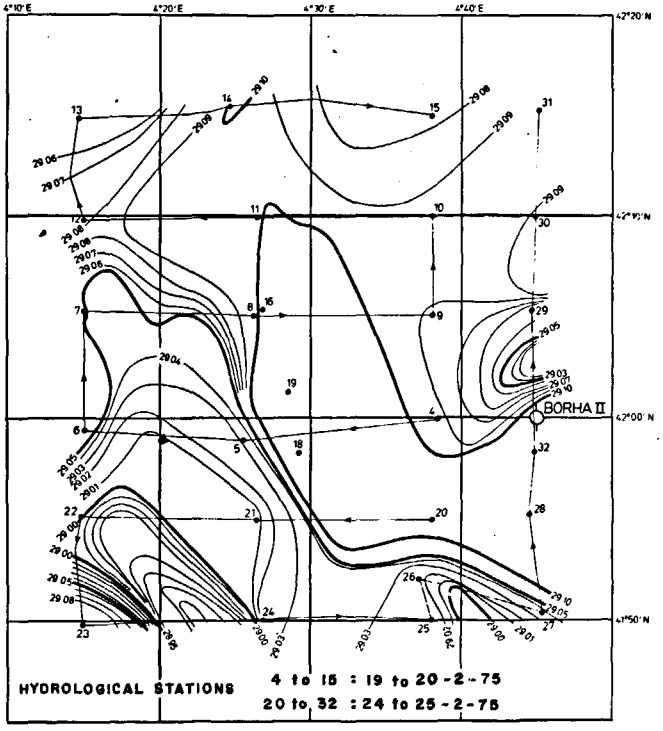

Figure 3
Surface Isopycnals (σ_θ).

Among the first group of stations (St. 4 to 16: 19-20 February), we observe very homogeneous water masses (St. 12 and 14) neighbouring stratified water masses (St. 13 and 15, fig. 4 A). In the western part of the zone, St. 6 clearly shows, in depth, cold water masses (Fig. 4 B).

Among stations 20 to 32 (February 24-25) warm water masses were present in depth, particularly at St. 21, 25, 26 (Fig. 4 B). There was a considerable amount of intermediate water between 100 and 400 m, at St. 25.

Using these data, including thermosalinograph surface data, we drew both surface and 150 m isopycnals (Fig. 3 and 5). At the surface there is a front, parallel to the line between St. 16, 20 and 28. At 150 m, the front vanishes in the North, but is still well defined in the southern part, between St. 26 and 25. It is then possible to estimate its slope (of the order of 1 %). At St. 16 to 20, which were done within 24 hours, a relatively homogeneous water mass is present from the surface to a depth of 1 000 m ($\theta \simeq 12{,}92°C$, $S°/_{oo} \simeq 38.455$; $\sigma_\theta \simeq 29.105$). The same water mass is present at St. 28 (Fig. 4 A), and at the "Bouée-Laboratoire" St. 15_B (Fig. 6).

The front separates dense, homogeneous and relatively warm waters to the North from more stratified light waters to the South. The "Bouée-Laboratoire" is situated during this period in the dense water zone.

We have some informations concerning the horizontal motions of these water masses at different depths, from the trajectories of 4 Swallow floats at 600 to 1 000 m in depth (Fig. 5) (Jeannin, 1976; Du Chaffaut, Tillier, Gascard, 1974). They drift towards the S-SE (8-10 cm.sec^{-1}) roughly parallel to the intersection of the front with the surface (Fig. 3). On 26 February, 2 floats were replaced in the center of the zone, near the site of the previous stations 8 and 16 (floats F4 and F5, Fig. 5). They then drift S-W, one at a depth of 800 m, the other at 1 000 m, towards previous St. 6. Two stations (33 and 35), situated just above floats F4 and F5, on 27 and 28 February, and separated by a distance of 15 km from each other, show a hydrological structure which resembles that at St. 6 (Fig. 4 B). In depth, there is cold water, which moves along the trajectory defined by the floats.

SECOND PERIOD: 27 FEBRUARY-12 MARCH

In late February, we observe a complete change in the hydrological situation at the "Bouée-Laboratoire". As shown by St. 17 B to 22 B (Fig. 6 A), the 3-layer stratified system is now present (Fig. 6 B). This new structure is announced by a sudden change of the horizontal velocity

Figure 4 A et B
Vertical profiles of potential temperature (θ°C).

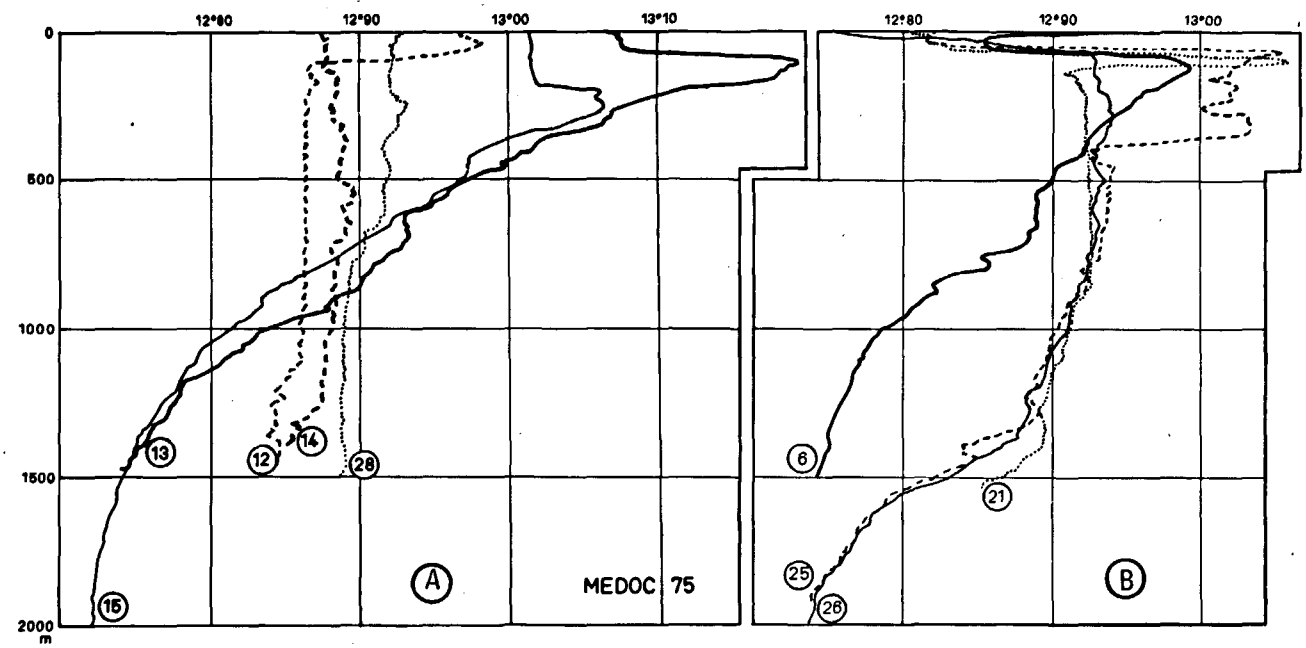

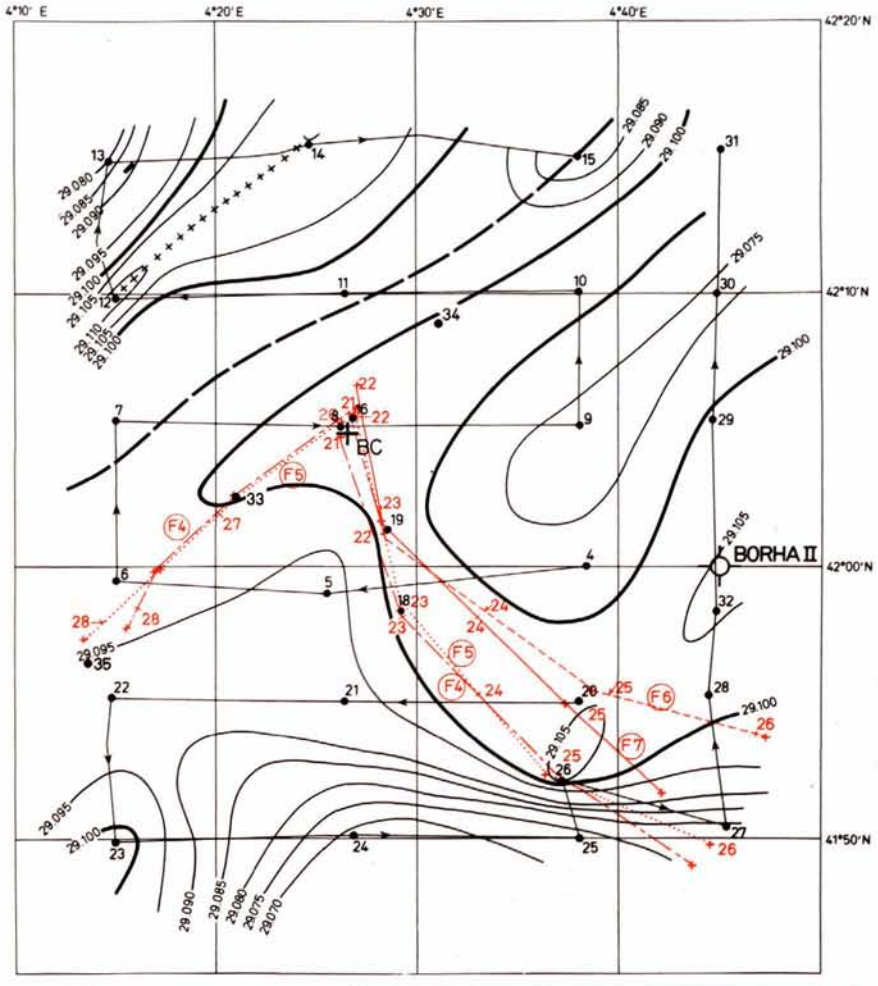

Figure 5
Isopycnals (σ_θ) *at* 150 *m depth from* 19 *to* 25 *February* 1975. *Horizontal float drifts from* 21 *to* 28 *February* 1975.

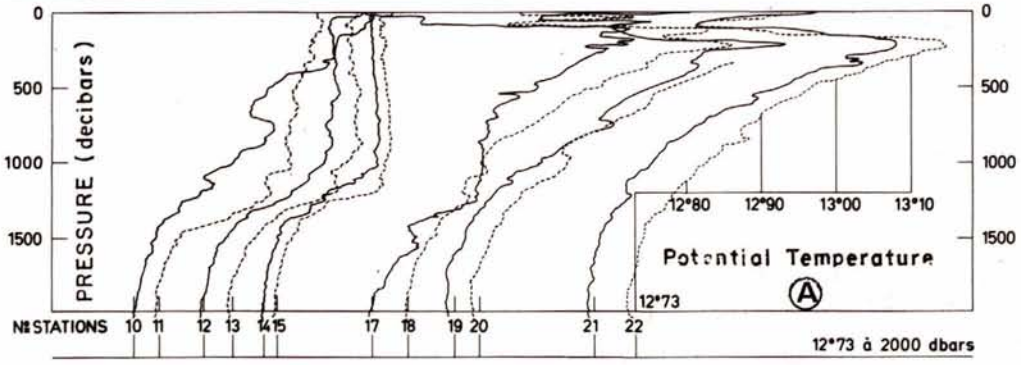

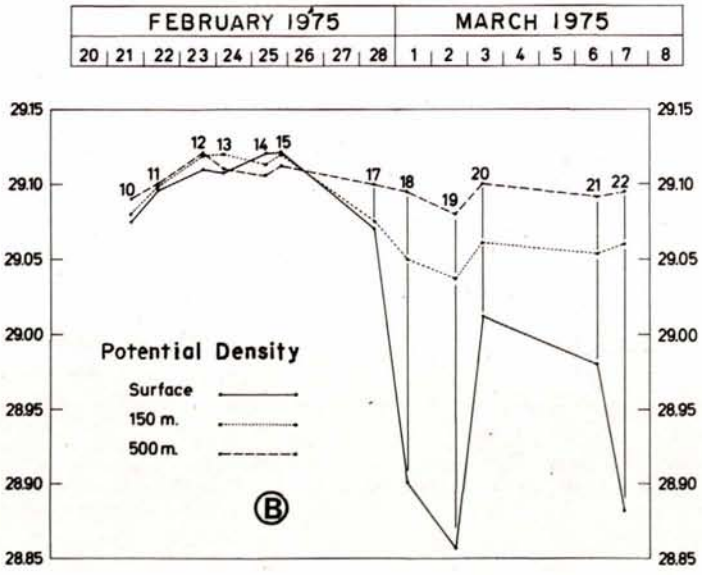

Figure 6
"*Borha II*": *Hydrological stations* 10_B *to* 22_B *from* 21 *February to* 7 *March* 1975. A, *vertical profiles of potential temperature;* B, *potential density change at three levels.*

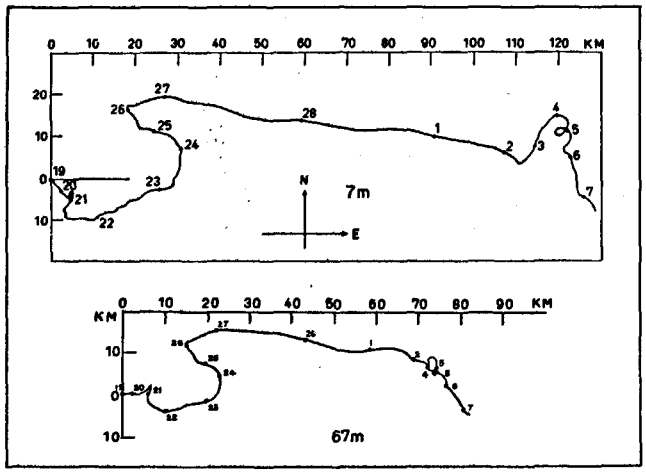

Figure 7
Progressive vector diagrams at 7 and 67 m depth from 19 February to 7 March 1975.

of the near-surface current measured at the "Bouée-Laboratoire" (7 and 67 m), which reaches almost 1 knot on 28 February (Fig. 7). It is interesting to note that the wind did not blow during this whole period.

In early March, a cyclonic eddy, 10 km in diameter, appears. It is centered at about 42°06'N-4°31'E, 12 n. miles N-W of the "Bouée-Laboratoire". At the same time, an anticyclonic circulation appears, centered 20 km to the West of the center of the cyclonic eddy (Fig. 8).

Four floats drifting at depths of 600, 800, and 1 000 m reveal the presence of the cyclone and anticyclone at these depths.

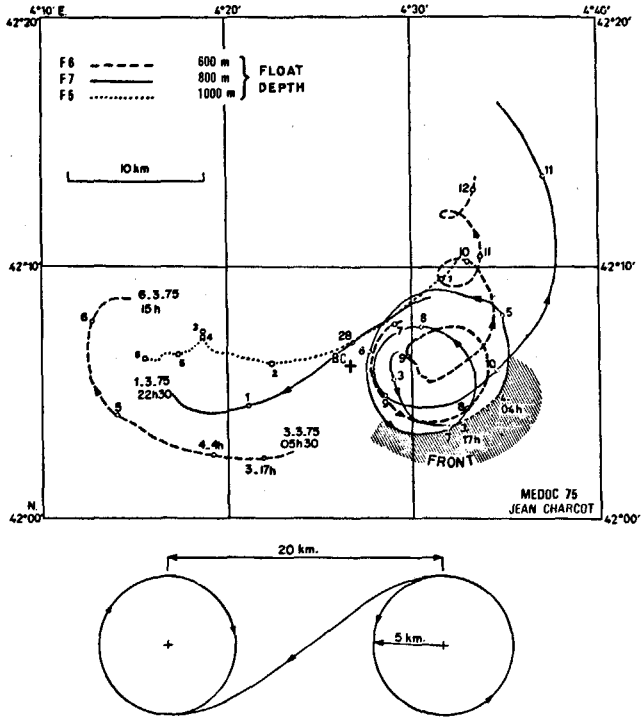

Figure 8
Horizontal float drifts from 27 February to 12 March 1975.

The floats drift approximately 5 km from the center of the eddy at a tangential speed of 10 to 15 cm . sec^{-1}, and a revolution is completed in about 3 days. Indeed, from March 2 to 8, the float F7, at 800 m depth, completes 2 revolutions.

Figure 9 A shows the potential temperatures θ and the

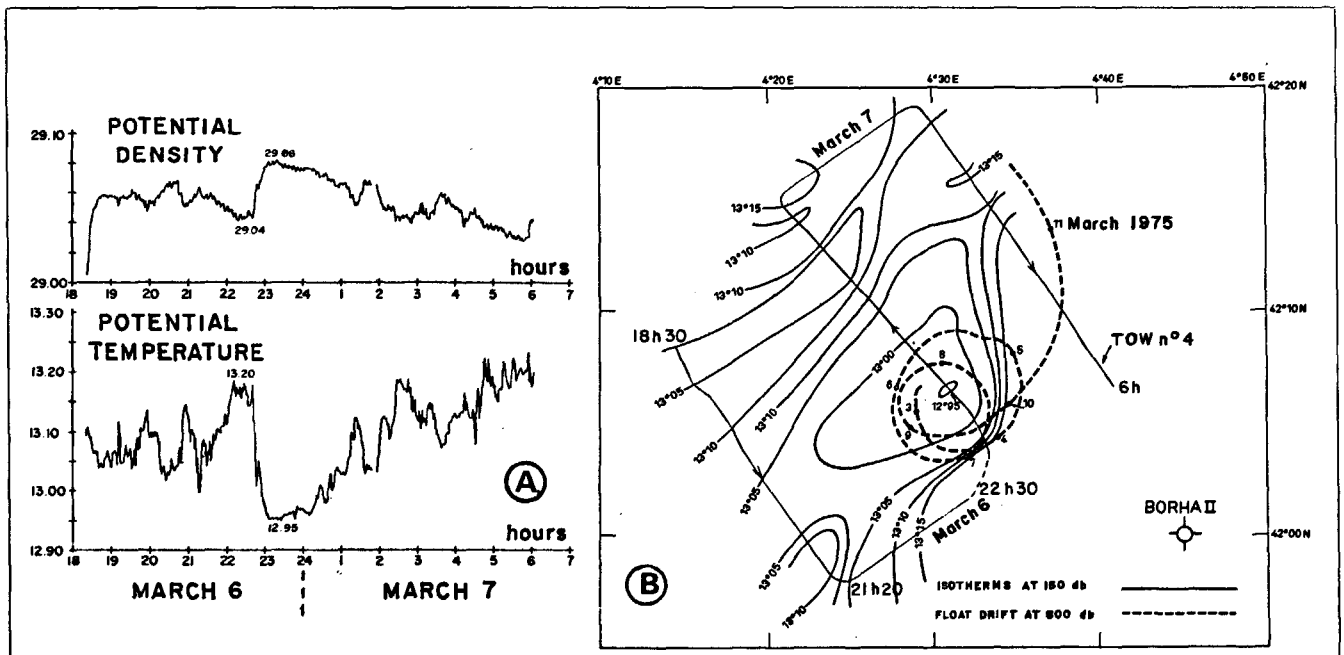

Figure 9
Bathysonde tow n° 4 on 6 and 7 March 1975. A, potential temperature and density computed from towed bathysonde data at about 150 m depth; B, potential temperature horizontal section at 150 m depth. Horizontal Float drift F_7 at 800 m depth from 2 to 11 March 1975.

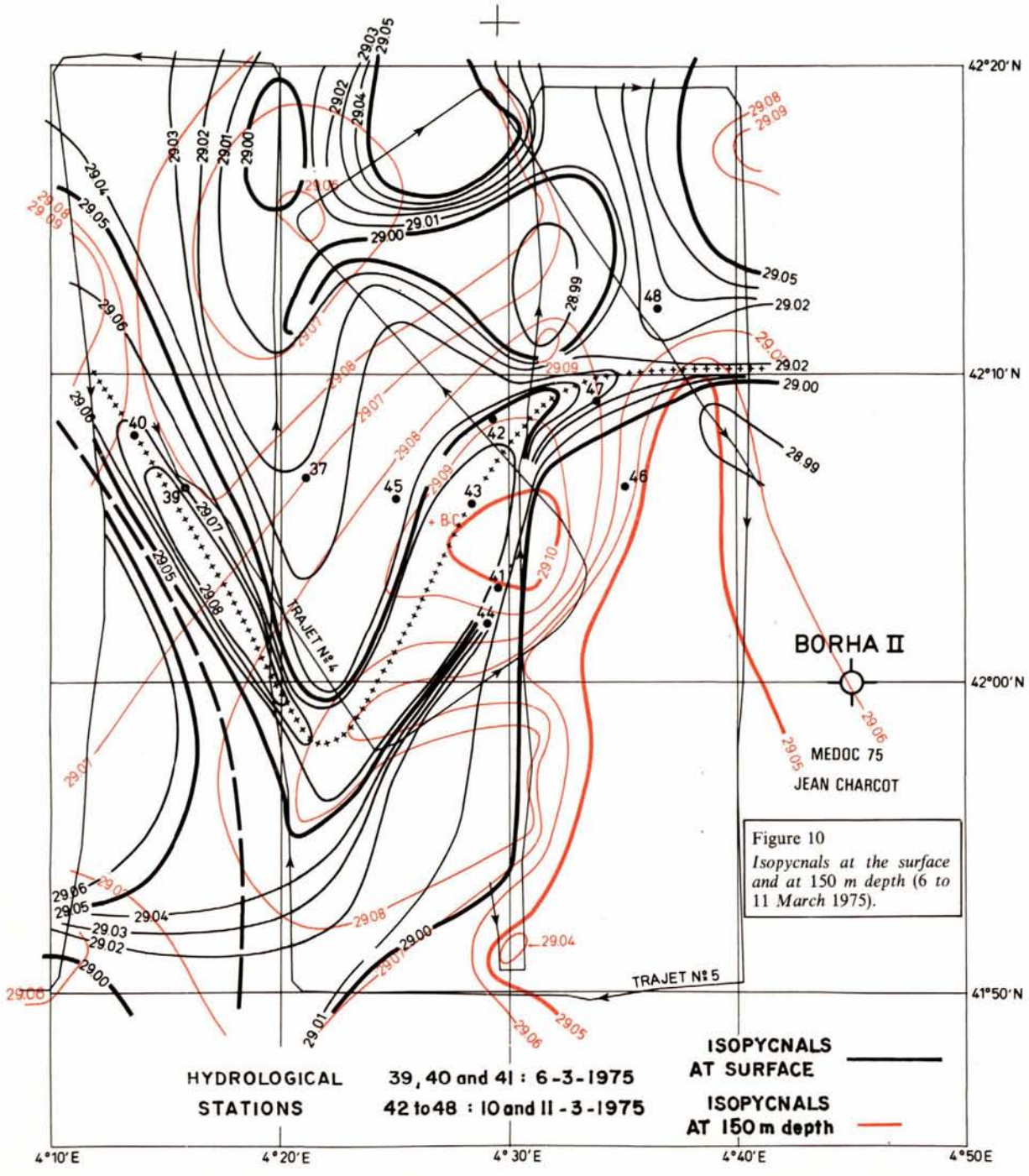

Figure 10
Isopycnals at the surface and at 150 m depth (6 to 11 March 1975).

densities σ_θ at 150 m depth, obtained from towed bathysonde data (Tow No. 4). A step both in density (29.04 to 29.08) and potential temperature (13.20 to 12.95°C) indicates that the bathysonde is crossing the front at 11 pm on March 6. At a depth of 150 m (Fig. 9 B), the front isotherms are well correlated with the cyclonic trajectory of the float at 800 m. At St. BC located on the western side of the cyclone (Fig. 8) four current-meters, between 300 and 2000 m, show the presence of the cyclone at these depths. *It appears likely that the cyclone exists from the surface down to the bottom.*

Comparison of the horizontal distribution of isopycnals at 0 and 150 m (Fig. 10) shows that the front, at the surface, is situated just above the center of the area limited by the isopycnal $\sigma_\theta = 29.10$ at 150 m, which corresponds to the center of the eddy at that depth. This phase-shift towards the West as a function of depth agrees with the theoretical model (p. 323).

On 9 March, after a long, quite uncommon period of calms, a Mistral gale begins and lasts for 36 hours. The eddy, which was stationary from March 2 to 9, is strongly modified. Once the wind starts to blow, loops appear in the float drifts at 600 m (Fig. 8) and 1000 m, and the cyclonic eddy migrates northwards at about 5 cm . sec^{-1}. Thus the cyclonic eddy, initiated and surviving during calm weather, rapidly decays after the onset of the Mistral. Many other observations: "Atlantis II" and "Discovery" during Medoc 69, (Voorhis, Webb, 1970; Caston, Swallow, 1970) show that such eddies probably exist permanently in a nascent state and are typical of the dynamics of this area in winter.

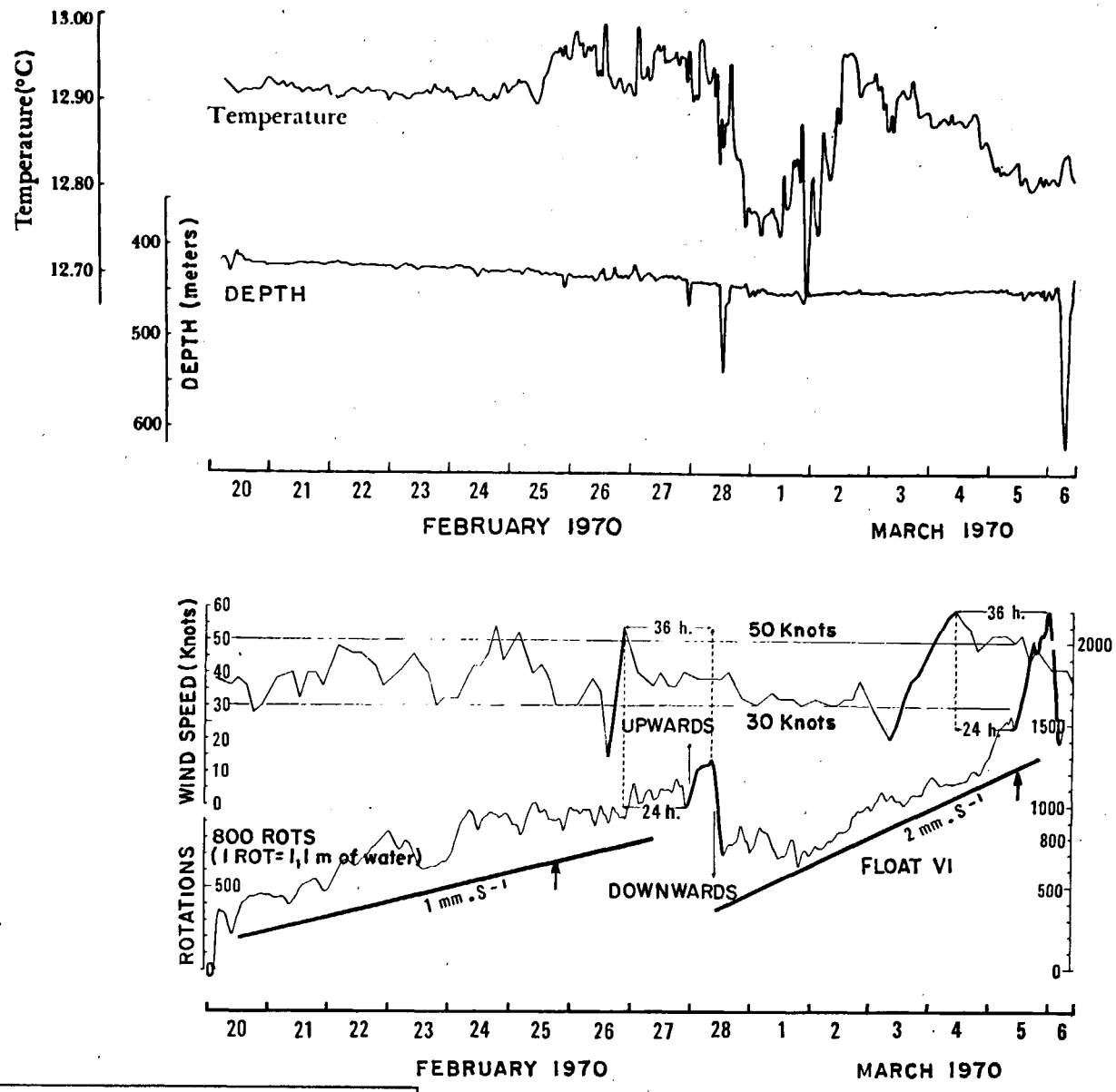

Figure 11

Water vertical motions at about 420 m depth observed nearby 42°N-4°20'E and Wind speed measured at Borha I (42°14'N-5°35'E) from 20 February to 6 March 1970.

As will appear from the model presented (p. 323) below, this cyclogenesis is significant of a baroclinic instability phenomenon.

Vertical motions of Medoc 70

During Medoc 70, with our colleagues Stommel, Voorhis and Webb we were able to measure the vertical component of motions within the interior of the fluid using the VCM technique (Webb, Dorson, Voorhis, 1970). Figure 11 shows the record of vertical velocities at 420 m depth within an area close to 42°N-4°20'E from 21 February to 6 March 1970. The figure also shows the wind speed measured at 20 m above sea level, at the "Bouée-Laboratoire Borha I" (42°14'N-5°35'E).

Three orders of magnitude of the vertical velocities are clearly revealed, which correspond, respectively, to

- an aperiodic and slow motion (1-2 mm.sec^{-1}) directed upwards in Figure 11, which characterizes an ascent of intermediate water masses. Since these water masses drift horizontally at about 10 cm.sec^{-1} speed, they move along a 1-2% slope, which is comparable to the slope of the front;
- inertio-gravitational internal waves. Such waves are very common in winter in this region. Then, their mean characteristics are an amplitude of a few hundred meters and a periodicity of several hours. The weaker the

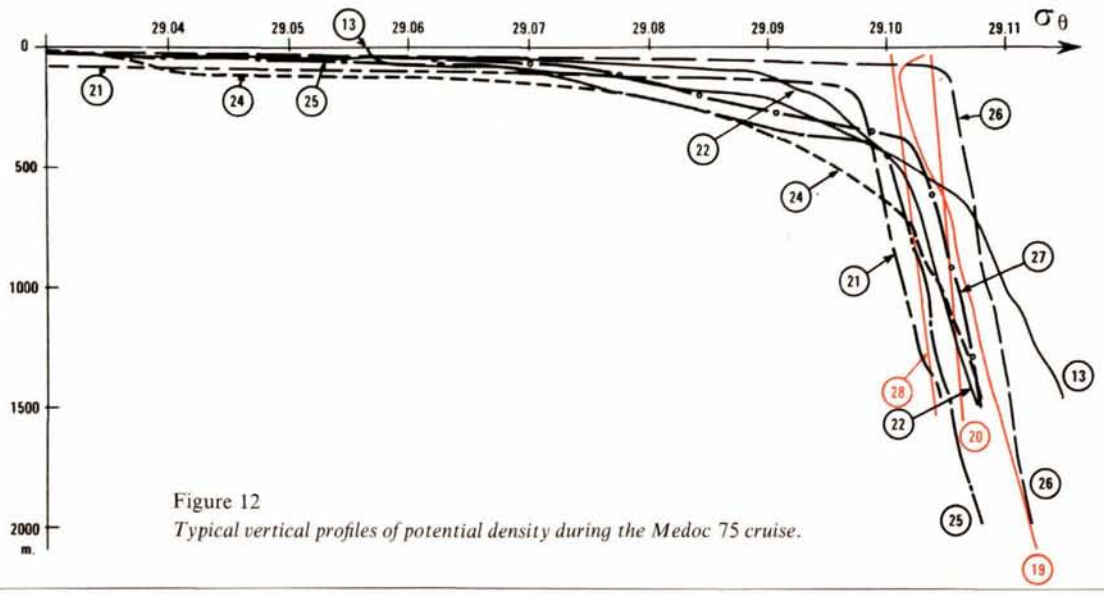

Figure 12
Typical vertical profiles of potential density during the Medoc 75 cruise.

stratification, the longer the period, and the greater the amplitude of these waves. Their vertical speeds are of the order of cm . sec^{-1} (Gascard, 1973). In Figure 11, these waves appear superimposed on the slow and aperiodic motion described above.

• intense convective motions. These are noticeable in Figure 11 as short and very strong peak velocities which may reach the highest ever recorded downwards vertical velocities (up to 10 cm . sec^{-1}.) They seem to follow peak values of wind (50-60 knots) quite regularly, 24 to 36 hours later.

We have very few examples of such high vertical velocities which can only occur over very short periods of time in very narrow places where the fluid is initially almost homogeneous. Theoretical models (Saint-Guily, 1972) in fact show that a perturbation of the surface density or surface velocity of a quasi-homogeneous fluid can trigger internal waves of several hundred meters amplitude, which may finally break.

According to these models, intense vertical motions could likely be triggered by winds into cyclonic eddies, where vertical stratification is very weak.

Slow and aperiodic motions and intense convective motions induce positive vertical heat fluxes.

In the first case, the intermediate water is convecting heat towards the surface.

In the second case, the intense downwards motion is followed by a large decrease of potential temperature from 12.88 to 12.68°C.

Then, we may state that two different kinds of phenomena contribute to the formation of deep waters.

MODEL OF BAROCLINIC INSTABILITY

Model

Our observations clearly show that, usually, surface and subsurface layers (0-500 m) are, on the one hand, more vertically stratified than deep layers (500-2 300 m), and that, on the other hand, there is an important shear in these surface layers (baroclinic layer) when motion in the deep layers is slow and uniform (barotropic layer).

Figure 12 shows vertical profiles of potential density at the several stations represented in Figure 3. It may be clearly seen that certain stations are characterized by a pycnocline, while others show uniform stratification from surface to bottom (no pycnocline). For these latter stations, and also for the former ones, except for the first 500 m which are more stratified and sheared, the mean gradient of potential density between 500 and 2 000 m is close to 5×10^{-9} m^{-1}. The mean depth D is close to 2 300 m around stations 4 to 32 (Medoc 75) and for $\partial\rho_\theta/\partial z = 5\times10^{-9}$ m^{-1} at this latitude $\varphi = 42°$N, $f = 10^{-4}$ sec^{-1}, and for quasi-homogeneous stations, we get, for the internal radius of deformation:

$$R_d = ND/f = 5 \text{ km}, \qquad N \simeq 2\times10^{-4} . \text{sec}^{-1}.$$

What is remarkable is that the R_d value is very close to that of the radius of the cyclonic eddy (Fig. 8).

In regions structured into two layers, the upper well stratified layer may be characterized by its thickness H_1 and its Brunt-Väisälä frequency N_1, higher than that of the lower layer N_2 with a thickness H_2.

From the profiles of Figure 12, it may be seen that

$$N_1H_1 \simeq N_2H_2 \simeq ND \simeq 0.5 \text{ m.sec}^{-1}.$$

From the outer stratified to the inner homogeneous region, the internal radius of deformation remains constant, despite the fact both the frequency N and the depth H (as well as the velocity gradient) are quite different. Thus, in the lower deep layer (H_2, N_2), the shear is very weak, practically close to zero considering the accuracy of our measurements. This appears clearly

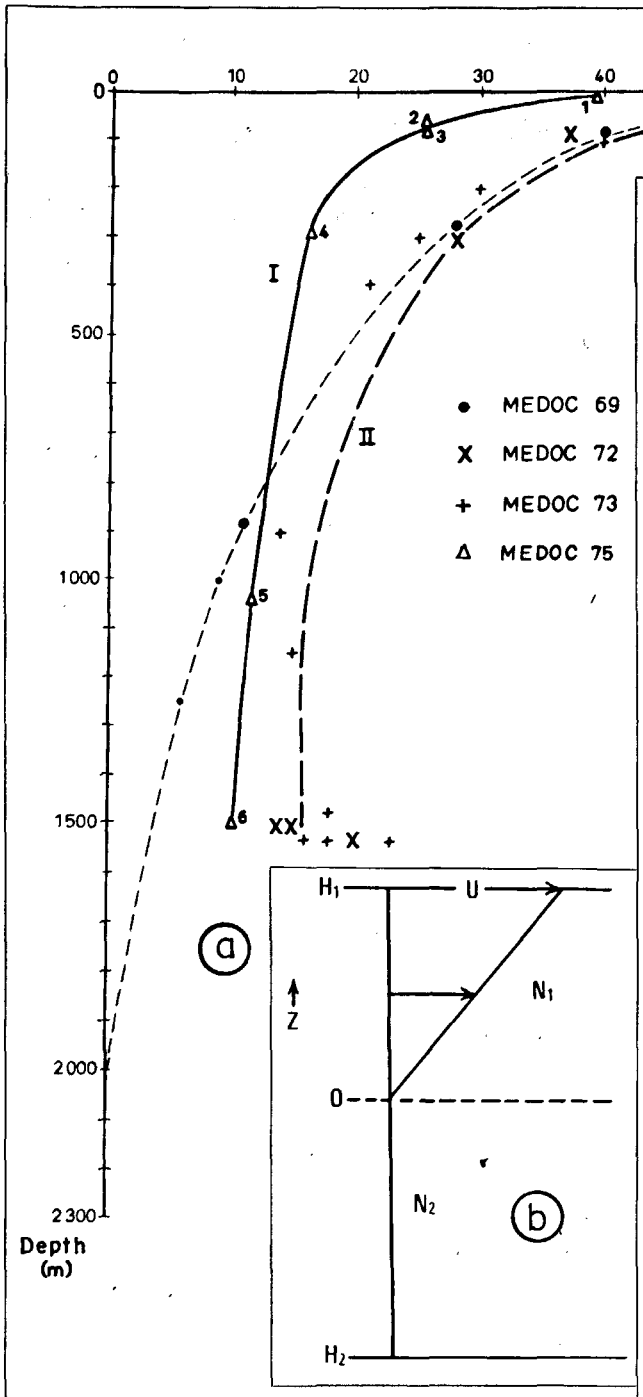

Figure 13
a, *typical vertical profiles of horizontal mean speed in Medoc area;*
b, *theoretical speed vertical profile.*

(Fig. 13 *a*) from current measurements made at the "Bouée-Laboratoire" at 7 and 67 m during Medoc 75 and from similar measurements made by "Discovery" during Medoc 69 (Gould, Larby, 1971) and from current-meters moored at station B_C (Medoc 75) at 350, 650, 1 050 and 1 650 m. All this is represented on profile I, where the maximum speed at the surface is 40 cm . sec^{-1}.

In the following model, we will consider between surface $z=H_1$ and bottom $z=-H_2$, an intermediate depth $z=0$ from which the geostrophic velocity increases linearly from 0 to U up to the surface. Below this depth $z=0$, the speed remains zero (Fig. 13 *b*).

For $0<z<H_1$, $\psi_1=-U.zy/H_1$.

We will consider a perturbation (meander) characterized by the function $\Psi'(x, z, t)$ with $-H_2<z<H_1$ and a vertical velocity $w'(x, z, t)$ which combines itself with the geostrophic streamfunction Ψ. The total function Ψ of the disturbed fluid linearised with respect to the fluid in the basic state is written for a small amplitude perturbation:

– in the upper layer:

$$\Psi_1=-\frac{U\,zy}{H_1}+\Psi'_1(x, z, t),$$

– in the lower layer:

$$\Psi_2=\Psi'_2(x, z, t),$$

with

$$u=-\partial\Psi/\partial y=U\,z/H_1$$

and

$$v=\partial\Psi/\partial x=\partial\Psi'/\partial x.$$

We will use the quasi-geostrophic approximation, since the Rossby number R_0 is of the order of 0.1 ($R_0=40\times10^{-2}$ m.sec$^{-1}/10^{-4}$ sec^{-1}.40×10^3 m) for these perturbations corresponding to 40 km wavelength meanders as mentioned in the Introduction. The quasi-geostrophic vorticity equation

$$(\partial/\partial t+U(z)\,\partial/\partial x)\,\nabla^2\Psi'=f_0\frac{\partial w'}{\partial z}$$

and the thermodynamic equation

$$\frac{\partial}{\partial t}\left(\frac{\partial\Psi}{\partial x}\right)+U(z)\frac{\partial}{\partial x}\left(\frac{\partial\Psi}{\partial z}\right)+v\frac{\partial}{\partial y}\left(\frac{\partial\Psi}{\partial z}\right)+\frac{N^2}{f_0}w'=0,$$

$$\frac{\partial}{\partial t}\left(\frac{\partial\Psi'}{\partial x}\right)+U(z)\frac{\partial}{\partial x}\frac{\partial\Psi'}{\partial z}-\frac{dU}{dz}\frac{\partial\Psi'}{\partial x}+\frac{N^2}{f_0}w'=0.$$

Let us try solutions for Ψ' such as

$$F(z)\exp(ik(x-ct)),$$

$$w'=f(z)\exp(ik(x-ct)),$$

$F(z)$ and $f(z)$, complex functions;
c, phase velocity, may be then written

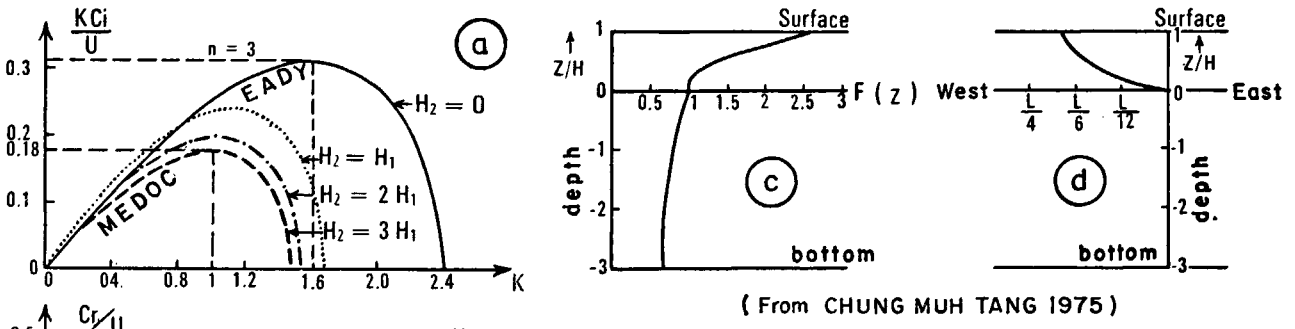

Figure 14

a, *growth rate and* b, *Phase speed of baroclinic unstable waves as a function of non dimensional wave number* K *and depth ratio* H_2/H_1. *Baroclinic unstable wave vertical structure for* $K=1$ *and* $H_2/H_1=3$. c, *wave amplitude* F(z) *(non dimensional);* d, *wave Phase shift.*

$$c=\frac{U}{2}\left\{1-\frac{n\,\mathrm{th}K_1}{K_1(1+n)}\right\}\pm\frac{U}{2}\left\{\frac{K_1-\mathrm{th}K_1}{K_1(1+n)}\sqrt{\Delta}\right\},$$

with

$$n=\frac{N_1}{N_2},\qquad K_1=k\frac{N_1H_1}{f}=K_2=k\frac{N_2H_2}{f},$$

$$\Delta=(n+a)\,(n+b),\qquad a=\frac{2(K_1/2-\mathrm{th}K_1/2)}{K_1-\mathrm{th}K_1},$$

$$b=\frac{2(K_1/2-\coth K_1/2)}{K_1-\mathrm{th}K_1}.$$

HORIZONTAL STRUCTURE. MEANDERS

Unstable modes appear when c has an imaginary part, that is when $\Delta<0$.

$n+a$ is always positive because K_1 is always greater than $\mathrm{th}\,K_1$ and a is thus always positive. On the contrary, $n+b$ may become negative and the instability criterion is written

$$n+b_0=0,$$

condition for which a cut-off frequency appears, separating an unstable region from a stable one.

Replacing b by its value, this condition is

$$\frac{2\coth K_0/2-K_0}{K_0-\mathrm{th}\,K_0}=n=\frac{H_2}{H_1}$$

with

$$K_0=k_0\,ND/f_0,$$

k_0 = cut-off wave number.

When the lower layer H_2 (Fig. 14 *a*) appears and increases as the upper layer decreases, so that $H_1+H_2=D=\mathrm{Cte}$:

1) the cut-off wavelength L_0 increases:

2) the growth rate of the wave of maximum instability decreases;

3) the wavelength of this wave of maximum instability is such as K tends to 1.

Then,

$$K=k\frac{ND}{f_0}=k\,R_d=1,$$

$$L=2\pi\,R_d=6.3\,R_d$$

For $R_d=5$ to 7 km, L is about 30 to 40 km.

This is in good agreement with the wavelength of meanders observed in Winter in the Medoc area.

For $H_2/H_1=3$, the exponential growth rate is

$$\sigma=k\,c_i=0.18\;U/R_d.$$

With $R_d=5$ km and $U=40$ cm . sec^{-1}, $\sigma=1.44\times10^{-5}$:

$$T=2\pi/\sigma=4.36\times10^5\ \mathrm{sec}=5\ \mathrm{days}.$$

This means that the *e*-folding time for the wave characterized by $L=6.3\,R_d$ is 3.5 days.

The phase speed of unstable waves (real part of c) which is equal to U/2 for $H_2=0$ and $H_1=D$, decreases when H_2/H_1 increases.

For $H_2/H_1=3$ and for $K=1$ (wave of maximum instability) this phase speed is

$c=U/5$ (Fig. 14 *b*).

VERTICAL STRUCTURE. PHASE SHIFT

The vertical structure of these unstable waves may finally be deduced from this model. To reach this result, general solutions for F(*z*) should be brought in the expression

of Ψ'. This calculation has been made by Tang (1975). Results are shown in Figure 14*c, d*, in the case of $H_2/H_1=3$ with $N_1H_1=N_2H_2$ for the wave of maximum instability ($K=1$). In Figure 14*c*, the amplitude $F(z)$ of Ψ' is normalized to its surface value. The amplitude is maximum at surface, decreases down to interface $z=0$, and decreases again slightly down to the bottom $z=-H_2$.

In the case of a basic current flowing West-East, the phase shift is westwards from interface $z=0$ up to the surface where it reaches, in distance units, one- sixth of the wavelength, i.e. a length close to the internal radius of deformation.

This agrees quite well with the observations which show that, at the surface, the front, which may be identified with surface streamlines, passes through the vertical of the center of the cyclonic eddy revealed by the float drifts at depths between 600 *m and* 1 000 *m* (*Fig.* 10).

POTENTIAL AND KINETIC ENERGY OF PERTURBATION: VERTICAL MOTION

The vertical gradient of potential density $\partial\rho_\theta/\partial z$ determines a characteristic horizontal scale for perturbations triggered by this instability mechanism. This scale is a function of the internal radius of deformation equal to H (disturbed fluid thickness) multiplied by the ratio of N (Brunt-Väisälä frequency) to f (Coriolis frequency).

The horizontal gradient of density $\partial\rho/\partial y$ implies a vertical shear. The perturbation growth rate is a linear function of this gradient.

This density field implies that a source of potential energy due to the slope $\gamma=(\partial\rho/\partial y)/-(\partial\rho_\theta/\partial z)$ of isopycnic surfaces is available to feed baroclinic instability.

We will now show both from theory and observations how this mechanism takes available potential energy from the mean current to create perturbation available potential energy and transforms it into perturbation kinetic energy K′ and perturbation potential energy A′. Killworth (1976) noted that horizontal shear can also have a great effect on growth rates and eddy positions.

Let us consider the linearised thermodynamical energy equation for the quasi-geostrophic perturbation

$$\frac{\partial\rho'}{\partial t}+U(z)\frac{\partial\rho'}{\partial x}+v'\frac{\partial\rho(y)}{\partial y}+w'\frac{\partial\rho_0(z)}{\partial z}=0.$$

Let us multiply each term by $g\rho'/-(\partial\rho_0/\partial z)$ which represents in geopotential units, the vertical displacement due to the perturbation of the isopycnal $\rho_0(z)$ from its original place in the basic state.
We get

$$\frac{g\rho'}{-\partial\rho_0/\partial z}\frac{d\rho'}{dt}+g\rho' v'\frac{\partial\rho/\partial y}{-\partial\rho_0/\partial z}-gw'\rho'=0,$$

$$\frac{d}{dt}\frac{g\rho'^2}{2(-\partial\rho_0/\partial z)}=-g\rho' v'\gamma+g w'\rho'.$$

This is the perturbation potential energy equation which is a very important relation.

The first term dA'/dt represents a variation of the perturbation potential energy $A'=g\rho'^2/2(-\partial\rho_0/\partial z)$ as a function of time. On the right-hand side of the energy equation, the second term $gw'\rho'$ is the exact opposite of the perturbation kinetic energy production rate $\partial K'/\partial t=-gw'\rho'$.

It thus represents a conversion of potential energy into kinetic energy of the perturbation. In the case of instability, amplifying perturbation, K′, must increase with time.

So $w'\rho'<0$. Then, for instance $w'>0$ (ascent) corresponds to $\rho'<0$.

w' indicates a conversion of potential to kinetic energy this does not mean an increase of the total perturbation energy. In the case of this perturbation being unstable, its potential energy A′ and its kinetic energy K′ should increase simultaneously. There should be then a production of available perturbation potential energy and more, this production rate should be higher than the conversion rate of potential energy into perturbation kinetic energy.

The production rate is expressed by

$$\frac{\partial A'}{\partial t}+\frac{\partial K'}{\partial t}=-g\rho' v'\gamma.$$

So

$$w'\rho'<v'\rho'\gamma,\qquad \frac{w'}{v'}=\delta<\gamma,$$

δ is the meridian slope of the trajectory followed by the disturbed water masses.

The production and conversion rates are maximum when $\delta=\gamma/2$.

Figure 15
Horizontal float drifts and hydrological station positions from 20 *February to* 2 *March* 1969.

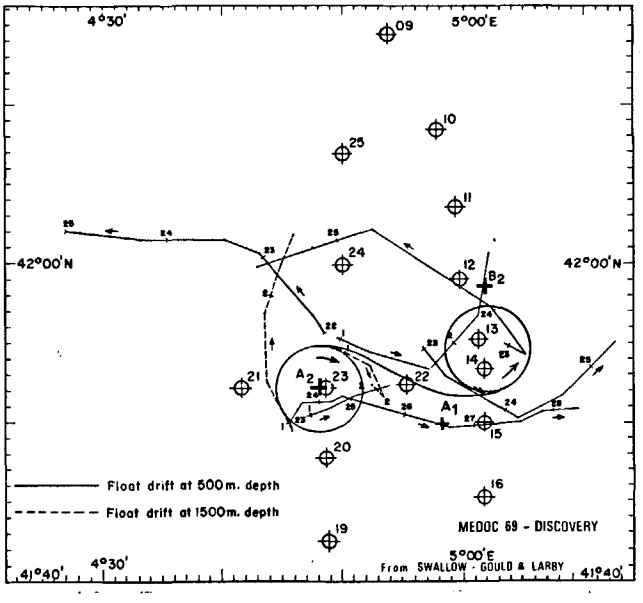

This result is confirmed by "Atlantis II" and "Discovery" Medoc 69 observations of the hydrological structure and three-dimensional motions. We are now presenting the "Discovery" observations, since they closely resemble those of Medoc 75. Indeed Figure 15 clearly reveals cyclonic and anticyclonic eddies similar to those presented in Figure 9. On a North-South hydrological section (Fig. 16) which intersects the cyclone (Fig. 15), we will note from station 16 to stations 10 and 11, an ascent of intermediate water from 200 m up to the surface. The maxima of temperature 13.19°C and salinity 38.48°/oo, observed at 190 m at station 16, are found at 10 m (13°C-38.46°/oo) at station 11, 19 nautical miles further North. This corresponds to a mean slope of 0.5%.

Figure 16

Hydrological meridian vertical section along 5°E from 25 to 28 February 1969.

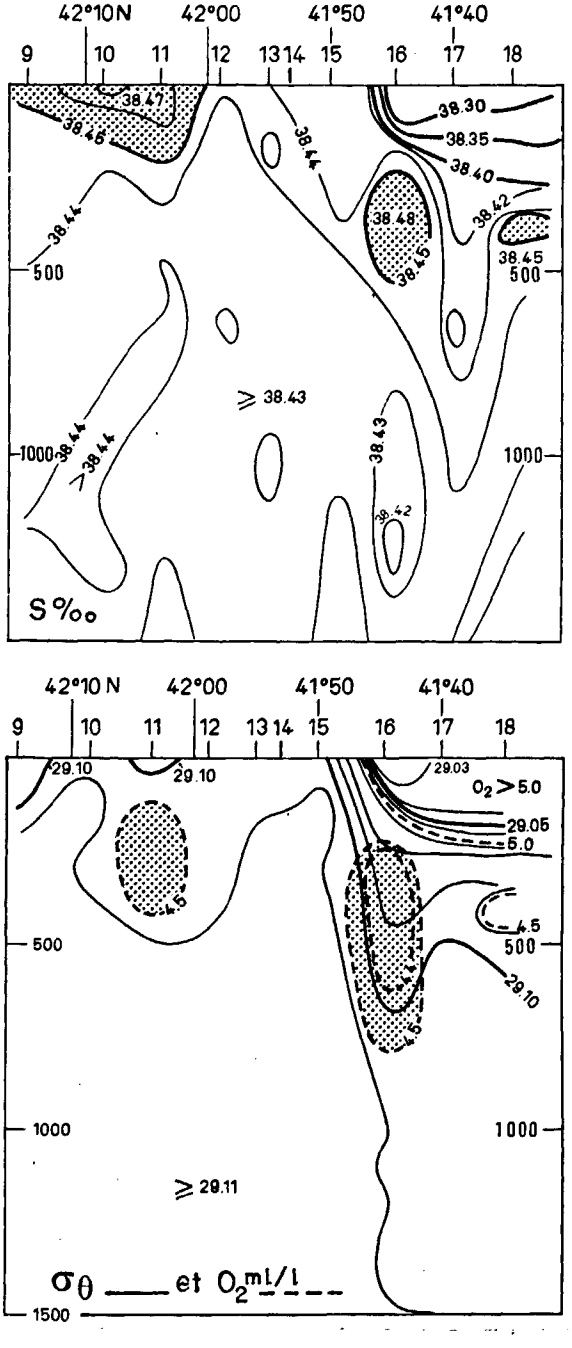

This ascent of intermediate water, which drifts northwards horizontally, leaving the cyclonic eddy to its left, is also confirmed by the dissolved oxygen (O_2) content of waters from stations 9 to 18. The intermediate water is poor in dissolved oxygen compared to ambiant waters, and may be traced from the O_2 minimum. This minimum is present at stations 16 and 11, at different levels, and the slope of the corresponding line is close to 0.5%. According to a positive meridian velocity of 15 to 20 cm.sec^{-1}, this mean slope corresponds to a positive vertical speed of 0.7 to 1 mm.sec^{-1}. The intermediate water thus requires two to three days to reach the surface.

Figure 16 also shows that, in the front region, the slope of isopycnals is significantly higher (1%) than the intermediate water slope. This front appears at about 41°45N and is characterized by a change in surface σ_θ from 29.03 to 29.10 corresponding to 38.30°/oo < S < 38.40°/oo and 12.60°C < θ < 12.95°C.

Three-dimensional general description of baroclinic unstable motions

We know from meteorology that baroclinic instability is a very active phenomenon in the atmosphere in the region of the polar front. This instability leads to the formation of cyclones and anticyclones, a well-known feature of the climate in extratropical regions.

There is great similarity between the dynamic behaviour of air masses along the polar front and the behaviour observed in water masses along the front which delineates the Medoc vortex. The latter extends horizontally over one degree of latitude while the northern atmospheric planetary vortex, limited approximately by the 40°N parallel, extends over 100°. Air masses move (10 m.sec^{-1}) a hundred times faster than water masses (10 cm.sec^{-1}) and the typical horizontal wavelength of meteorological perturbation resulting from this instability mechanism (4000 km) is a hundred times greater than the Medoc meander wavelength (40 km), each one depending of an internal radius of deformation respectively 700 to 800 km in the former case and 5 to 8 km in the latter. Since the height of the disturbed fluid is of the order of 10 km in the atmosphere and 1 km in the ocean, one may deduce that the vertical gradient of potential density is 100 times smaller in the ocean (Medoc area) than in the atmosphere. So the similitude ratio between the atmospheric and oceanic phenomena is thus close to 100.

The main difference is due to the β effect, important in the atmosphere but negligible in the case of the ocean, relative vorticity advection being much larger than planetary vorticity advection for short wavelength perturbations (short in comparison with the earth radius).

Thus, when considering baroclinic instability in the ocean, we may describe the three-dimensional motions of the fluid induced by this mechanism in a way similar to the atmosphere (Palmen, Newton, 1969) (Fig. 17) and the following description explains most of our observations.

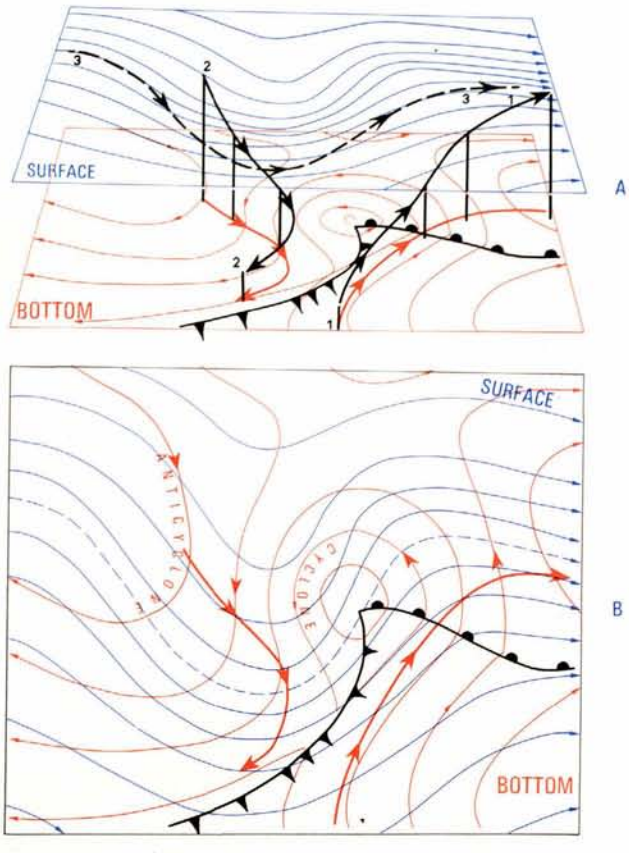

Figure 17

A, *Block diagram and* B, *horizontal projection of the three-dimensional motions of water masses within a state of baroclinic instability in relation with surface and bottom streamlines.*

In case of instability, an initial small perturbation is amplifying and an anticyclonic (cyclonic) tendency then increases at the ridge (trough). Since vorticity advection is zero at the ridge (trough), a horizontal divergence (convergence) appears, as shown by the quasi-geostrophic equation. This in turn induces a positive (negative) vertical motion at the ridge (trough).

This explains how subsurface waters (1) move upwards at the meander ridge. At the trough, for similar reasons, surface waters (2) move downwards.

Surface divergence: deep cyclone

At the ridge near the surface, the vertical motions of water masses (1) decrease and horizontal motions increase. These waters are subjected to shrinking since their thickness decreases and the conservation of their potential vorticity implies a positive anticyclonic tendency. In other words, the ridge is amplifying, the surface horizontal divergence increases and positive vertical motions increase. Deeper waters must be converging horizontally to feed on this upward motion, and this induces a *cyclonic circulation* close to the bottom friction layer.

A deep cyclone thus appears just below the surface ridge.

Surface convergence: deep anticyclone

Upstream to the surface perturbation trough, water masses (2), north of the front in Figure 17, are subsiding. Initially, their horizontal component of motion decreases, while the vertical component increases, so that water masses (2) are stretching and their potential vorticity conservation implies a positive vorticity tendency which reinforces the trough. Getting deep, close to the bottom friction layer, the vertical motion of water masses (2) decreases. These waters are shrinking and then, by the same conservation law, an *anticyclonic circulation* appears.

South of the front, light water masses (3) begin to subside with waters (2), but since they are much less dense, they begin to move upwards once they pass the trough. They then meet with waters (1) at the ridge, where they mix. *This intermixing by advection of these two types of waters is very efficient and plays an important rôle in the formation of the thick mixed layer.*

Ultimately two deep fronts appear which are similar to warm and cold fronts well-known to meteorology. One is formed in front of subsiding dense waters (2), and the other in front of rising intermediate waters (1). As they cross fronts, streamlines intersect, resulting in a drastic change in current directions which is a typical feature appearing in a progressive vector diagram of horizontal currents observed in the Medoc area.

MEDITERRANEAN DEEP WATER FORMATION

We saw that baroclinic instability plays a very important rôle in the processes of mixing and transformation of superficial and intermediate waters into deep waters. According to this fact, we will now describe a new model for Mediterranean deep water formation in the North-Western Basin. This model is developed in *three phases*, and its evolution in space and time is described in *three successive stages*.

The three phases

PRECONDITIONING PHASE

During this phase, the effects of cooling and evaporation on the surface waters lead to an increase in density so that a convective motion starts, the vertical amplitude of which is all the more important as the density increase in surface is great, or the superficial layer stratification is weak. This convection involves a turbulent vertical mixing and, progressively, a homogeneous mixed layer appears below the surface. The thickness of this layer increases with time; the surface cooling and mixing being supposed constant, the growth rate slows down, while the thickness of the layer increases. In a cyclonic circulation, this vertical *convective mixing* is able to erode the central stratification faster than the peripheric one.

The slope $\gamma = (\partial\rho/\partial y)/(-\partial\rho_0/\partial z)$ of the isopycnals, which separates the central waters of low stability from the surrounding stratified waters, increases with $\partial\rho/\partial y$; this results in an increase of the shear velocity between the two layers. When γ reaches values of about 1 %, the general cyclonic circulation becomes unstable and the process of baroclinic instability may start. This process flattens the "doming", while meteorological conditions at the surface tend to reinforce it.

BAROCLINIC INSTABILITY PHASE

The first elements of that instability phenomenon are "meanders" in the cyclonic circulation of surface layers, that is, perturbations of the mean trajectory of the 3-layer stratified waters around the dense and quasi-homogeneous central vortex. This vortex, with a radius of about 30 nautical miles, is centered at 42°N-5°E. The mean horizontal scale of meanders is 40 km. We were not able to know how many meanders may appear simultaneously around the vortex. Teledetection measurements, with a resolution of 1/10° in temperature and 1 km in horizontal distance, would give a good idea of the whole phenomenon in surface. It is possible that 6 to 8 meanders may appear at a time for the meander wavelength is approximately equal to the vortex radius. Killworth (1976) predicted 8 to 14 eddies !

The meanders are accompanied by an upward motion of intermediate water, compensated by downward motion of dense waters, with velocities of about 1 mm . sec^{-1}. These vertical motions associated with the perturbation involve cyclonic and anticyclonic eddies 10 km in diameter. They are coupled and their centers are 20 km apart, which corresponds to a half perturbation wavelength. There is thus a ratio close to 2 π (as we demonstrated p. 323) between the wavelength of the meanders and the internal radius of deformation (6 km).

MIXING PHASE

At the vortex periphery, baroclinic instability involves a progressive transformation of water masses by inter-mixing of surface and subsurface waters. This results in a slow horizontal and vertical spreading of the central mixing zone. Progressive cooling and evaporation, which occur permanently in winter during periods of calm, act on this quasi-homogeneous mixing zone and induce a slow downward motion of new homogeneous and dense waters, once the doming structure of the isopycnals reaches a new state of baroclinic instability. This is the first process of deep waters formation. We call it the *advective process.*

Otherwise, strong and sudden surface cooling and evaporation produced by the "Mistral" or the "Tramontane" acting on such a quite homogeneous and unstable structure will trigger intense and deep convection within the interior of the fluid. This results in the formation of a second type of new deep waters. We call it the *convective process.*

The three stages

First stage: mixing between 0 *and* 200 *m*

Formation of a Winter surface water and of a subsurface layer of minimum temperature above the intermediate water layer.

Under the effect of cooling and evaporation, the temperature of surface waters decreases and salinity increases so that, by convective mixing, they become homogeneous over 100 to 200 m. In the center of the circulation, a cold "winter surface water" (density close to 1.029) appears. Its characteristics vary from one winter to another, but its mean values are: $\theta \sim 12.60$°C, S‰ ~ 38.10 and $\sigma_\theta \sim 28.90$. It is formed at the periphery of the vortex and the central homogeneous and dense zone progressively extends. Then, by baroclinic instability, this "winter surface water" sinks beneath the surface water of the 3-layer system [mass (2), Fig. 17]. By this way, a temperature minimum appears in a layer above the intermediate water layer (which is characterized by a temperature maximum).

Second stage: mixing between 0 *and* 500 *m*

Disappearance if the intermediate water by mixing with the winter surface water and consequent increase in the sea surface temperature.

As soon as the upper part of the intermediate water [warm and salted water masses (1), Fig. 17] upwells and mixes with surface waters (3), the temperature of the mixing no longer decreases and its salinity increases. As more and more intermediate water becomes involved in the mixing, both its temperature and its salinity increase. This evolution is clearly illustrated by the θ-S diagrams (Gascard, 1977). Finally, a quasi-homogeneous water layer extends from the surface down to about 500 m.

Third stage: mixing down to the bottom and deep water formation

• First Process

The whole fluid column is then affected by the baroclinic instability mechanism. Cyclonic and anticyclonic eddies appear, extending from the surface down to the bottom. Old deep waters begin to upwell like masses (1) and mix with waters (3) (Fig. 17). Warm and salted waters resulting from the second stage mixing, which have been subjected during their surface stay to cooling and evaporation, downwell like masses (2). The mixing process then deepens quite rapidly as shown by station 28, Figure 4 A.

• Second Process

Since the vertical stratification now becomes very weak, the action of strong winds on the dense and homogeneous waters may be very efficient, and a very deep convection may result from sudden surface cooling. This effect produces a new kind of deep waters, the temperature and salinity of which are significantly lower than the new deep water resulting from the first process.

Rapid vertical convective motions up to 10 cm . sec^{-1} induce a very large horizontal divergence which cannot be compensated by a change in vorticity. The quasi-geostrophic equilibrium is then destroyed, which means that we are no more concerned with meso-scale motions produced by baroclinic instability, motions which are classified in the rotationnal subrange ($L > 10$ km), but with small scale phenomena in the buoyancy subrange ($L < 1$ km).

Ultimately, new deep waters of the first and second types can mix and form the Mediterranean deep water. Its mean characteristics, $\theta \sim 12.73$°C, S ~ 38.41‰, are remarkably constant. However, depending on winter meteorological conditions, one can observe from one year to another slight fluctuations around the mean, as more new deep waters of one type are formed at the expense of deep waters of the other.

CONCLUSION

In winter, in the North-Western Mediterranean Sea, we clearly observed a baroclinic instability of the cyclonic vortex centered at 42°N-4°45E, 100 km in diameter and 3 or 4 weeks circular period. At the periphery, the instability produces small size (10 km) and short period (3 days) eddies extending from the surface to the bottom. Through this instability mechanism, surface waters may mix with intermediate waters. Mainly triggered by heat fluxes or wind stresses at the surface, convective mixing occurs, characterized by intense vertical velocities of up to 10 cm . sec^{-1}. This convection penetrates as much deep as surface and subsurface layers are already mixed by advection due to baroclinic instability.

Thus, this double mechanism ultimately produces a very thick mixed layer which feeds on the deep layers with a new deep water. The deepening of this mixed layer may reach down to the bottom, if three conditions are met:

– cyclonic circulation (vortex);

– intermediate layer of warm and salted water at mid depth;

– meteorological forcing creating intense evaporation and cooling at the surface.

This explains why oceanic deep water formation only occurs in a very few places in the open ocean.

Small size eddies, similar to the "Medoc ones", have been observed in the Arctic Ocean (Newton, Aagaard, Coachman, 1974) and are probably induced by baroclinic instability (Hunkins, 1975; Hart, Killworth, 1976). A mixed layer results within the first hundred meters below the surface. But this layer cannot penetrate deeply because, initially, the intermediate water is too deep.

As for the Mediterranean in Winter, in the Labrador Sea, and in the Weddell Sea (Gordon, in press), the three conditions for deep waters formation are then present. Similar small eddies (few kilometers) exist together with very thick mixed layer (several thousands meters).

In many other parts of the ocean, these three conditions are sometimes more or less present. Since numerous large cyclonic eddies, similar to the Medoc vortex, exist in the open ocean, it would not be surprising to have to consider that advective and convective type of mixing such as that observed in the Medoc area frequently occurs in the formation of surface deep mixed layers. For example, might not the "18°C" North-Atlantic water (Worthington, 1959), which is quite homogeneous from the surface to 400 m, and the "Levantine Water" be formed in winter by this double mixing process?

Acknowledgements

This work was supported by the Centre National de la Recherche Scientifique (LA 175) and by the Centre National pour l'Exploitation des Océans.

REFERENCES

Anati D. A., 1971. On the mechanism of the deep mixed layer formation during Medoc 69, *Cah. Oceanogr.*, **23**, 4, 427-443.

Caston G. F., Swallow J. C., 1970. Neutrally buoyant floats, serial numbers 209-227, February-March 1969, tables and diagrams. National Institute of Oceanography, Int. Rep. n° D3.

Du Chaffaut M., Tillier P., Gascard J.-C., 1974. Acoustical localisation system for the tracking of underwater drifting floats. in *Ocean 74. IEEE int. Conf. Ocean Environment*, Halifax, 21-23 août 1974, **2**, New York, IEEE Publ., 139-144.

Gascard J.-C., 1973. Vertical motions in a region of deep water formation, *Deep-Sea Res.*, **20**, 11, 1011-1027.

Gascard J.-C., 1977. Quelques éléments de la dynamique de formation des eaux profondes méditerranéennes, thèse Doct. Sci. Phys., Univ. Pierre-et-Marie-Curie, Paris, 147 p.

Gordon A. L., Deep Antarctic convection West of Maud Rise, under press.

Gould W. J., Larby M. J., 1971. Moored current meter records, Medoc 69, Discovery cruise 25, January-March 1969, NIO mooring 028-037, National Institute of Oceanography, Int. Rep. n° A47.

Hart J. E., Killworth P. D., 1976. An open baroclinic instability in the Arctic, *Deep-Sea Res.*, **23**, 7, 637-645.

Hogg N. G., 1973. The preconditioning phase of Medoc 69, II. Topographic effects, *Deep-Sea Res.*, **20**, 5, 449-459.

Hunkins K. L., 1975. Subsurface eddies in the Arctic Ocean and baroclinic instability, *Climate of the Arctic*, 398-406.

Jeannin P. F., 1976. Medoc 75. Courantométrie à l'aide de flotteurs dérivants, Muséum Paris, Labor. Océanogr. Phys. Rap. Int.

Killworth P. D., 1976. The mixing and spreading phases of Medoc I, *Prog. Oceanogr.*, **7**, 2, 59-90.

Lacombe H., Tchernia P., 1972. Caractères hydrologiques et circulation des eaux en Méditerranée, in: *The Mediterranean Sea*, edited by D. J. Stanley, Dowden, Hutchinson and Ross, Stroudsberg (Pa.), 26-36.

Lacombe H., Tchernia P., 1972. Le problème de la formation des eaux marines profondes. Déroulement du phénomène en Méditerranée nord-occidentale par hiver très froid (janvier-mars 1963), *Ann. Inst. Océanogr.*, **48**, fasc. 1, 75-110.

Medoc Group, 1970. Observation of formation of deep water in the Mediterranean sea, *Nature*, **227**, 5262, 1037-1040.

Newton J. L., Aagaard K., Coachman L. K., 1974. Baroclinic eddies in the Arctic Ocean, *Deep-Sea Res.*, **21**, 9, 707-720.

Nielsen J. N., 1912. Report on the danish oceanographical expeditions 1908-1910 to the Mediterranean and adjacent seas. **1**. Hydrographical observations.

Palmen E., Newton C. W., 1969. *Atmospheric circulation systems*, Academic Press, New York, 603 p.

Saint-Guily B., 1972. On the response of the ocean to impulse, *Tellus*, **24**, 4, 344-349.

Sankey T., 1973. The formation of deep water in the North Western Mediterranean. in *Progress in Oceanography*, **6**, edited by B. A. Warren, Pergamon Press Oxford, 159-179.

Stommel H., Voorhis A. D., Webb D. C., 1971. Submarine clouds in the deep ocean, *Am. Sci.*, **59**, 6, 716-722.

Stommel H., 1972. Deep winter-time convection in the Western Mediterranean sea, in *Studies in physical oceanography. A tribute to Georg Wüst on his 80 th birthday*, edited by A. L. Gordon, Gordon and Breach, New York, **2**, 207-218.

Swallow J. C., Caston G. F., 1973. The preconditioning phase of Medoc 69. I. Observations, *Deep-Sea Res.*, **20**, 5, 429-448.

Tang C.-M., 1975. Baroclinic instability of stratified shear flows in the ocean and atmosphere, *J. geophys. Res.*, **80**, 9, 1168-1175.

Tchernia P., Fieux M., 1971. Résultats des observations hydrologiques exécutées à bord du N/O « Jean Charcot » pendant la campagne Medoc 69 (30 janvier-28 février), (18-31 mars), *Cah. océanogr.*, **23**, suppl. n° 1, 1-91.

Voorhis A. D., Webb D. C., 1970. Large vertical currents observed in a winter sinking region of the North Western Mediterranean, *Cah. océanogr.*, **22**, 6, 571-580.

Webb D. C., Dorson D. L., Voorhis A. D., 1970. A new instrument for the measurement of vertical currents in the ocean, in *Conference on electronic engineering in ocean technology*. University College of Swansea, 21-24 septembre 1970. 1ère Conf. Proc., n° 19, 323-331.

Worthington L. V., 1959. The 18° water in Sargasso Sea, *Deep-Sea Res.*, **5**, 4, 297-305.